RSC Advances

PAPER

View Article Online
View Journal | View Issue

Cite this: *RSC Adv.*, 2024, **14**, 38934

Preparation and properties of a novel alginate/carrageenan crosslinked coordination polymer and evaluation of the antibacterial, antioxidant and anticancer potential of its Co(II), and Cr(III) polymeric complexes

Maged S. Al-Fakeh, *[a] Nora S. Al-Subaie,[b] Yassine EL-Ghoul *[a] and Zeineb Hamden[c]

Natural polysaccharides play a crucial role across diverse fields such as medicine, food, and cosmetics, for their various physiochemical and biological properties. In this study, we developed a new crosslinked biopolymer using sodium alginate (AG) and carrageenan (CAR) polysaccharides. Various metal complexes involving different metal salts such as $CoCl_2 \cdot 6H_2O$ and $CrCl_3 \cdot 6H_2O$ were synthesized using the crosslinked biopolymer formed above. The two polymeric complexes were characterized using Fourier-transform infrared spectroscopy (FT-IR), elemental analysis, ultraviolet-visible spectroscopy (UV-Vis), magnetic susceptibility, molar conductivity techniques, and thermogravimetric analysis. The Co(II) polymeric complex exhibits a tetrahedral X-ray crystal structure and belongs to the monoclinic crystal system. Cr(III) complex is octahedral and crystal data are in compliance with the cubic crystal system. The antimicrobial study showed a significant activity improvement for all the developed complexes against both Gram-positive as well as Gram-negative bacterial pathogens – *Staphylococcus aureus*, *Microscus luteum*, *Escherichia coli* and *Salmonella typhimurium*. Similarly, the different polymeric complexes showed an efficient activity against *Candida albicans* as anti-fungal effect. Moreover, higher antioxidant values of the two complexes were obtained with DPPH scavenging activity ranging between 73% and 94%. In addition, both the polymeric complexes were subjected to biocompatibility cell viability assays along with *in vitro* anticancer evaluation. The alginate/carrageenan crosslinked coordination complexes revealed excellent cytocompatibility with normal human breast epithelial cells (MCF10A) and a high anticancer potential with human breast cancer cells (MCF-7) which increase significantly in a dose-dependent manner.

Received 21st September 2024
Accepted 3rd December 2024

DOI: 10.1039/d4ra06818a

rsc.li/rsc-advances

1. Introduction

A Coordination Polymer (CP) describes periodic structures that stem from the coordination bonding of metal entities and ligands. They can be designed to opt for the porous architectures described as Metal–Organic Frameworks (MOFs). Coordination polymers have good thermal stability so they can be employed in catalytic reactions such as oxidation of inert C–H bonds of hydrocarbons, hydrogenation of olefins, Knoevenagel condensation reaction, *etc.* The coordination chemistry of the metals involved plays a large role in their solubility and reactivity as the ore is refined into precious metal.[1,2] Many of the mechanisms of growth coordination polymers rely on self-assembly which entails the crystallization of a metal cation with a ligand. This can be done by employing crystallization and crystal engineering strategies that are already known. The forces that are considered to cause the molecules to arrange spontaneously (in this case, metal–ligand complexes), are considered to include van der Waals' forces, pi–pi interactions, hydrogen bonding, and stabilization of a molecule's pi bonds by polarized bonds besides the coordination bond between the metal and the ligand. The building blocks engage in coordination interactions and other relatively weaker interactions including hydrogen bonding in solution to form some other small molecular units; however, based on the self-assembly coordination polymers grow based on the same interactions.[3–5] Algae represent a viable and sustainable natural resource for the synthesis of a diverse range of renewable biopolymers. These seaweed biopolymers have shown to have excellent qualities

[a]*Department of Chemistry, College of Science, Qassim University, Buraidah 51452, Saudi Arabia*
[b]*Department of Chemistry, College of Science, University of Bisha, Bisha, 61922, Saudi Arabia*
[c]*Laboratory of Interfaces and Advanced Materials, Faculty of Sciences of Monastir, University of Monastir, Monastir 5000, Tunisia*

and a wide range of applications. In many fields related to medicine, food, cosmetics, and the environment, they are employed either directly or modified through chemical processing or combining, and as material reinforcement.[6–10] From the biomass of algae, various naturally occurring polysaccharides are extracted, including agar, laminarin, fucoidan, alginate, and carrageenan. They display a range of biological characteristics. In fact, they have demonstrated strong antimicrobial, antioxidant, antitumor, and immunomodulatory properties.[11–17] Alginic acid is a polysaccharide that has water soluble properties located in the cell walls of brown algae and forms viscous gum when it is in water-saturated condition. $NaC_6H_7O_6$, sodium alginate is a sodium salt of alginic acid. According to the method sodium alginate is a gum. Its salts with metals for example sodium and calcium are referred to as alginates. It is one of the major components of biofilms formed by the bacterium *Pseudomonas aeruginosa*, which is an opportunistic pathogen colonizing the lungs of certain individuals affected with cystic fibrosis[18] This biofilm and *P. aeruginosa* has a high resistance to antibiotics,[19] and are susceptible to inhibition by macrophages. Alginic acid is a straight chain polymer consisting of β-D-mannuronic acid (M) linked 1→4 to α-L-guluronic acid (G) by (1→4) linkages or alternatively the monomers can be linked in any sequences or blocks covalently. Sodium alginate is applied in different fields and industries such as food and animal feed, fertilizers, textile printing, and drugs.[20–24] Another property of dental impression material is that uses alginate as a way of gelling. Calcium alginate is allowed food-grade ingredient in food processing and manufactured foods.[25] Some may give a creamy consistency resembling alginate while others are hard to turn into a gel and their uses are based on technical aspects since color difference is irrelevant.[26] Carrageenan furthermore is classified as linear sulfated polysaccharide biopolymers that are extracted from red edible seaweeds. The most common uses are in food industries because of their gelling and thickening as well as stabilizing abilities. Their main use is in the dairy and meat sector because of their high affinity for food proteins. Carrageenan is produced in three different types depending on the extent of sulfation carried on the product. There are occasions when carrageenan acts as a vegetarian and vegan option to gelatin and on other occasions it can be used to substitute gelatin in confectionery. Carrageenan is a naturally extracted water-soluble polysaccharide obtained from reddish seaweeds belonging to the Rhodophycea class. It has been employed as a thickening, or gelling agent to control and prolong the release of the drug, in food and pharmaceuticals and many other applications.[27–30] Carrageenan and alginates because of their application properties *i.e.* thickening and gelling agents and their bioactivities antiviral, immune-inflammatory, and anticoagulant are used in pharmaceutical, cosmetics, and mainly food industries.[31] Carrageenan (CAR) is referred to as a general name of a class of the high molecular weight sulfated polysaccharides produced from red seaweed through extraction and formed by units of D-galactose and able 3,6-anhydrogalactose (3,6-AG) linked through α-1,3 and β-1,4 glycosidic bonds.[32] CAR is a sulfated polygalactan with ester-sulfate group content of 15–40%, which indicates that CAR is an anionic polysaccharide. In the food industry and particularly in milk products, CAR finds use as a gelling, stabilizing, and thickening agent as well as for fat replacement. They are also employed in other nonedible products such as cosmetics, pharmaceuticals,[33,34] textiles, formulations, and printings.[35] The objective of this research study is to take advantage of the benefits of crosslinking alginate and carrageenan polyanionic biopolymers having multiple binding sites and greater biological properties in addition to further enhance their effectiveness by complexing different metals. First, in the current study, we will use citric acid to crosslink a biopolymer of AG/CAR. Then both transition and non-transition metal-mixed ligand coordination polymers will be synthesized and their structures determined using various methods. Next, the physical, chemical, and biological activities of these metallic coordination polymers will be carried out. Last of all, cell viability studies employing normal human breast epithelial cell line (MCF10A) and human breast adenocarcinoma cell line (MCF-7) will be carried out to evaluate the *in vitro* biocompatibility and anti-cancer efficacy of the developed polymeric systems.

2. Experimental

2.1. Materials

The chemicals and reagents used in the study were of analytical grade as far as what was available was concerned. For the preparation of sodium alginate (AG-Na), a product with a 70% degree of deacetylation, medium viscosity, and average molecular weight of 30 000 g mol^{-1} was purchased from Sigma Aldrich, St Louis, USA. Furthermore, the citric acid was used as a crosslinking agent (CTR, 226. 2 g mol^{-1}), and carrageenan (CAR, fine-white powder) was purchased from Sigma-Aldrich.

2.2. An overview of characterization of polymer complexes

CHN determination for the prepared compounds was performed using an Analytischer Functions test element analyzer (VELP Scientifica Srl, Usmate (MB), Italy). FTIR spectral data was recorded in the range of 4000–400 cm^{-1} with an (ATR) on an infrared spectrophotometer-Gladi-ATR spectrophotometer from Agilent Technologies, Santa Clara, CA, USA. To ensure the association of the different measurements, the resolution used in the measurements was set to 4 cm. The magnetic moments of the prepared composites were determined with the help of a magnetic susceptibility (MSB-Auto) from Sherwood Scientific, Cambridge. UV/Vis electron spectra were obtained with a spectrophotometer, Shimadzu, UV-2101 PC, Kyoto, Japan in the wavelength range 200–700 nm. The conductivity of the complexes was determined by a conductivity meter obtained from Jenway Instrument Company, Model 4310, London, UK. TG/DTG studies of the complexes were conducted in dynamic air on the Shimadzu thermal analyzer (DTG 60-H, Kyoto, Japan) at the heating rate of 10 °C min^{-1}. At the temperature range of 20–600 °C. All X-ray diffraction patterns were recorded on a diffractometer designed by Philips, Eindhoven, The Netherlands, model PW 1720. Measurements were conducted on

complex polymer samples within the scan range of 10–90° and using steps of 0.01°. The Scherer eqn (1) was applied to estimate the average crystalline particle size of coordination polymers:

$$D = K\lambda/\beta \cos\theta \quad (1)$$

The Scherer eqn (1) was applied to estimate the average crystalline particle size of the coordination polymers: where K is the shape factor, α is the wavelength, β is the line that has been broadened at half maximum density in radian, θ is the Bragg angle and D is the average size of the crystalline arrangement. The morphology of the synthesized Co(II) and Cr(III) compounds was examined by SEM using a JEOL type microscope (JEOL JSM-5400 LV, JEOL Ltd., Akishima, Japan). Experiments were performed under a voltage of 5 kV.

2.3. Preparation of the crosslinked polymeric ligand (poly-AG/CTR/CAR)

First, in a round-bottomed flask 2 g of sodium alginate polymer is dissolved in 100 mL of purified water and stirred vigorously for 1 hour at a temperature of 80 °C. A dropwise carrageenan solution that previously prepared by dissolving 2 g of carrageenan in 100 mL of H_2O and heating it at 70 °C with constant stirring. Then leave for an hour. After that 2 g of the CTR crosslinking agent and stirred at 120 °C for 2 hours. The reaction will be stirred at 90 °C overnight. Then, the resulting suspension was cooled, to room temperature and concentrated under reduced pressure. The resulting product was dried at 60 °C under vacuum to obtain a stable white powder (90%).

2.4. Preparation of the polymeric transition metal compound

2.4.1. Preparation of the $[Co(AG\cdot CT\cdot CAR)(H_2O)_2]$ complex. Dissolve 0.2 g of $CoCl_2\cdot 6H_2O$ in 15 mL of H_2O (solution 1), then dissolve 0.8 g of Co in a mixture of ethanol/water (10/10 mL) (solution 2). The prepared solution 2 was heated at 70 °C for 15 minutes. After cooling to room temperature, the solution 1 was added while stirring continuously for 3 hours. Then we filter the precipitate and place it in a Petri dish in the oven for two days at a temperature of 50 degree Celsius. The final product obtained is a fine, pink-colored powder.

2.4.2. Preparation of the $[Cr(AG\cdot CT\cdot CAR)(H_2O)_3Cl]$ complex. We dissolve 0.40 g of $CrCl_3\cdot 6H_2O$ in 15 mL of distilled water (solution 1). Then we dissolve 0.8 g in an ethanol/water mixture (10/10 mL). The solution is heated at 70 °C for 15 minutes with constant stirring. After cooling to temperature, solution 1 of the metal is added with continuous stirring for 3 hours. A precipitate is formed, which is collected and dried in an oven for 24 hours at a temperature of 50 °C. We obtain a fine powder of dark green color.

2.5. Biological analysis

2.5.1. Antimicrobial activity. Antimicrobial activity screening was performed using the agar disc diffusion method.[36] For the antibacterial assay, we used two Gram-positive strains: *Staphylococcus aureus* ATCC 25923 (Sa) and *Staphylococcus aureus* NCIMB 8166 (Ml) and two Gram negative strains: *Escherichia coli* ATCC25922 (Ec) and *Salmonella typhimurium* ATCC 14080 (St). In the antifungal test, we used a pathogenic reference strain of yeast *Candida albicans* ATCC 90028 (Ca). The inoculums of the pathogenic bacteria and yeast strains were adjusted to 0.5 McFarland standard turbidity and then streaked onto Muller–Hinton (MH) agar plates using a sterile cotton mop. Sterile filter discs (diameter 6 mm, Biolife Italy) were placed on the surface of the agar mediums, and 20 μL of each polymeric complexes (ligand, Co(II) complex, Cr(III) complex) diluted in sterile dimethyl sulfoxide (DMSO 5%) at a concentration of 10 mg mL^{-1} was dropped onto each disc. After incubation at 37 °C for 24 h, the antibacterial activity was evaluated by measuring the inhibition zone formed around the disc. Each assay was performed in triplicate.

2.5.2. DPPH free radical scavenging activity. DPPH, the stable artificial free radicals, has been widely used for the measurement of free radical scavenging capacity of the compounds in ethanol and aqueous systems.[37] Briefly, 2 mL DPPH solution (0.2 mM, in 95% ethanol) was incubated with 2 mL different of polymeric complexes (ligand, Co(II) complex, Cr(III) complex) solutions at a concentration of (10 mg mL^{-1}). Then, the reaction mixture was shaken and incubated in the dark for 30 min at room temperature. The absorbance was immediately recorded at 517 nm against ethanol with a spectrophotometer (Metash, model UV-5200, Shanghai Xiwen Biotech. Co., Ltd, Shanghai, China. The DPPH free radical scavenging rate was calculated using the equation and expressed in % of scavenging:

$$\text{DPPH scavenging activity (\%)} = [1 - (\text{abs sample}/\text{abs control})] \times 100$$

2.5.3. Cell viability and anticancer assays. MCF-10A which is a normal human mammary epithelial cell line and MCF-7 which is a human breast cancer cell line was purchased from American Type Cell Culture, Manassas, Virginia, USA. Growth medium for all cells included Dulbecco's Modified Eagle's medium with a solution derived from fetal bovine serum and containing both penicillin (100 IU mL^{-1}) and streptomycin (100 μg mL^{-1}) as antibiotics. The culture medium was further maintained at 5% CO_2 and 100% relative humidity at 37 °C. The anticancer activity and the cell viability assays were conducted using the MTT tested standardized tetrazolium with some modifications.[38] Cell culture was then done in a 96-well plate with 2 × 10 cells per well added for each plate to be treated. Culture media containing samples at different concentrations were added to each of the cell cultures after 24 h of incubation. After 72 hours of incubation, we go for an MTT assay. Indeed, the treatment with MTT solution (1 mg mL^{-1} in culture medium named RPMI 1640 supplemented with 10% fetal bovine serum and 10 μg mL^{-1} antibiotic: 5 μg mL^{-1} penicillin and 5 μg mL^{-1} streptomycin) began after 48 h of incubation. The appearance of purple formazan crystals from the yellow tetrazolium salt was an indicator of metabolically active cells. To calculate the percentage of survival of these cells, we used

the ratio (OD in the test group/OD in the control group × 100), which was measured using an ELISA reader at 570 nm after 2 h of incubation in an incubator at 37 °C with 5% CO_2. Three independent experiments were performed.

3. Results and discussion

3.1. Preparation of the different polymeric compounds

Poly-AG/CTR/CAR polymeric ligand was firstly prepared by reacting the two AG and CAR biopolymers with citric acid as a crosslinking agent. The crosslinked polymer, poly-AG/CTR/CAR, was synthesized as a result of the polyesterification reaction, which occurred between the carboxylic groups of the CTR and the hydroxyl groups of the carrageenan on the one hand, and between the CTR and hydroxyl groups of the alginate biopolymer on the other. The Co(II) and Cr(III) coordination complexes were created through the reaction of the poly-AG/CTR/CAR with the two metal salts. The poly-AG/CTR/CAR's capacity for binding the two metals is due to the various reactive groups present in the alginates, carrageenan, and CTR of the crosslinked polymer. The two polymeric complexes react in a molar ratio; of 1 : 1 (metal cations: SO^{4-} from CAR or COO^{-} from AG). These various compounds were inert to air and did not dissolve in water and in most organic solvents with the exception of DMSO. for this purpose, conductivity measurement of various complexes (10^{-3} M) was carried out in the DMSO solvent. The molar conductivity values of Co(II) and Cr(III) metal complexes were 4.00 and 10.93 A m S cm^2 mol^{-1}, and 93 A m S cm^2 mol^{-1}, respectively. Various additional characteristics of the ligand and the different complexes such as color, elemental resolution, decomposition point, and conductivity are shown in the Table1.

3.2. FT-IR analysis

The FT-IR spectra data of the main peaks is shown in Table 2. In relation to the polymeric ligand's synthesis, we can observe the appearance of a new band at about 1712 cm^{-1}, which indicates the ester group's creation, by comparing the spectra of the ligand and the alginate or carrageenan biopolymer. This ester formation occurred between the hydroxyl groups of the glycosidic moiety of the alginate and carrageenan biopolymers and the carboxylic groups of the CTR, which was used as a crosslinking agent. Thus, we deduce that the CTR crosslinking agent served as an intermediary in the polyesterification reaction that produced the polymeric ligand between the alginate and carrageenan (Fig. 1). Additionally, the ligand band, which correlates to the OH stretching, appears at approximately 3431 cm^{-1}. Simultaneously, a strong band close to 1035 cm^{-1} emerges which is related to the C–O–C stretching vibration of the glycosidic structure.[39] The characteristic band at 1000–1100 cm^{-1} due to glycosidic C–O–C bond, stretching vibration of the pyranose ring is shown at 783 and 560 cm^{-1}. Looking at the various spectra of the complexes in comparison to the polymeric ligand alone, we can observe some apparent shifts, especially at 3431 cm^{-1} (ν O–H), 1725 (ν O–H), and 1260 cm^{-1} (ν S=O). The evident interactions between the metal and the corresponding groups in the polymeric ligands were the origin of these wavenumber shifts. In polymeric linkages, there are various absorbances displayed for carrageenan sulfate groups which include sulfate (1214 cm^{-1}), galactose-4-sulfate (920 cm^{-1}), and galactose 2-sulfate (834 cm^{-1}).[40] The band

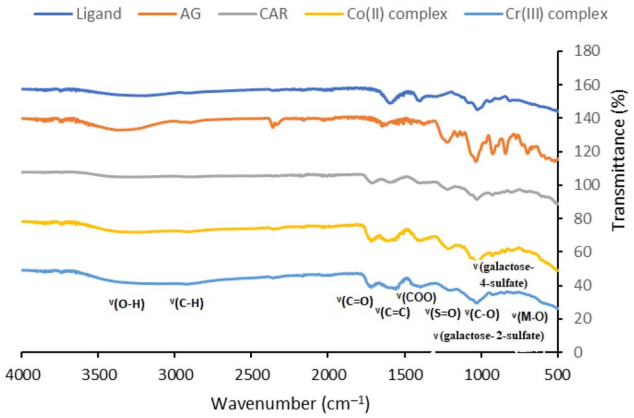

Fig. 1 FT-IR spectra of the alginate, carrageenan, polymeric ligand (poly-AG/CTR/CAR), and the different prepared Co(II), and Cr(III) coordination complexes.

Table 1 Color, elemental analysis, and decomposition point of the mixed ligand complexes

			Found (calc.%)				
Complex	M.F (M. Wt)	Color	C	H	S	M.p. (°$C_{Decomp.}$)	A m S cm^2 mol^{-1}
Ligand	$C_{24}H_{27}O_{26}S_2$ (795.37)	Beige	36.92 (36.23)	3.76 (3.42)	8.52 (8.06)	110	—
$[Co(AG{\cdot}CTR{\cdot}CAR)(H_2O)_2]$ **1**	$C_{24}H_{29}O_{28}S_2Co$ (888.53)	Pink	32.60 (32.44)	3.42 (3.29)	7.18 (7.22)	198	4.00
$[Cr(AG{\cdot}CTR{\cdot}CAR)(H_2O)_3Cl]$ **2**	$C_{24}H_{31}O_{29}S_2CrCl$ (935.06)	Dark-Green	30.95 (30.82)	3.52 (3.33)	6.60 (6.85)	185	10.93

Table 2 FT-IR spectral bands of the ligand and its metal compounds

Compound	ν(O–H)	ν(C–H)	ν(C=O)	ν(C=C)	ν(C–O)	ν(S=O)	ν(–C–H)	ν(=C–H)	ν(M–O)
Ligand (poly-AG/CTR/CAR)	3431	2177	1725	—	1035	1260	560	783	—
$[Co(AG/CTR/CAR)(H_2O)_2]$	—	2925	1650	—	1026	1213	889	926	522
$[Cr(AG/CTR/CAR)(H_2O)_3Cl]$	3249	2917	1650	1593	1027	1200	—	925	520

Table 3 UV-Vis spectra and magnetic moments values of the ligand and its metal compounds

Complex	V_{max} (cm^{-1})	Assignment	$\mu_{eff.}$ (BM)
Ligand (poly-AG/CTR/CAR)	24.213	n → π*	—
	39.215	π → π*	
[Co(AG/CTR/CAR)$(H_2O)_2$]	27.548	n → π*	4.35
	35.211	π → π*	
	21.645	d–d transition	
[Cr(AG/CTR/CAR)$(H_2O)_3$Cl]	28.818	n → π*	3.94
	34.247	π → π*	
	21.786	d–d transition	

emerging at 505–516 cm^{-1} for the Co(II) and Cr(III) complexes was attributed to (H_2O) to support the coordinated water (ν M–O).[41] We can infer that the hydroxyl, carboxylic, ester, and sulfate groups of the synthetic poly-AG/CTR/CAR biopolymer, are able to coordinate with the different metal ions and are primarily function in a bidentate configuration.

3.3. UV-Vis spectrophotometric analysis

UV-Vis spectra of the complexes formed with DMSO solvent were as follows, Table 3; As-prepared spectral bands were found at 24 213 and 39 215 nm that are assigned to the n → π* and π → π* transitions in the CAR and AG biopolymers.[30] Characteristic bands of the Co(II) complex were found at 27 548 nm, 35 211 nm and 21 645 nm. From the latter it appears that the bands correspond to n → π* transition, π →π* transition, and $^4T_{1g}(D) \rightarrow {}^6A_{1g}$ transition accordingly. For the Cr(III) complex, the typical bands were assigned at 28 818, 34 247 & 21 786 nm corresponding to n → π*; π → π* & $^4T_{2g}(G) \rightarrow {}^6A_{1g}$ respectively. The various characteristic bands of Co(II) and Cr(III) complexes in the visible region have been assigned to d–d transitions common in octahedral metal complexes.[42,43]

3.4. Magnetic moments

At room temperature, the magnetic moment values for complexes (1–4) are shown in Table 3. The results are as follows: values indicating, their possible formations as polymer–metal compounds. In fact, the Co(II) magnetic-moment was 4.35 BM, a value that shows a high-spin d5 system with 5 unpaired electrons tetrahedral formation around Co(II).[42] As for the Cr(III) magnetic-moment, measuring the magnetic moment revealed a value of 3.94 BM, which indicates the formation of high-spin d6 Cr(III) ions with 5 unpaired electrons in their appropriate outer valence shell. The octahedral arrangement around Cr(III).[43] The suggested structures for the complexes are shown (Fig. 2) as follows.

3.5. Thermogravimetric Analysis

Analytical TGA and DTA data concerning different ligands and polymers are presented in Fig. 3 and Table 4, respectively. In the case of Co(AG/CTR/CAR)$(H_2O)_2$, the thermal curves are composed of four major decomposition stages that take place within the temperature range of 80–125 °C, 127–214 °C, 216–398 °C and 400–500 °C. The first step is characterized by the

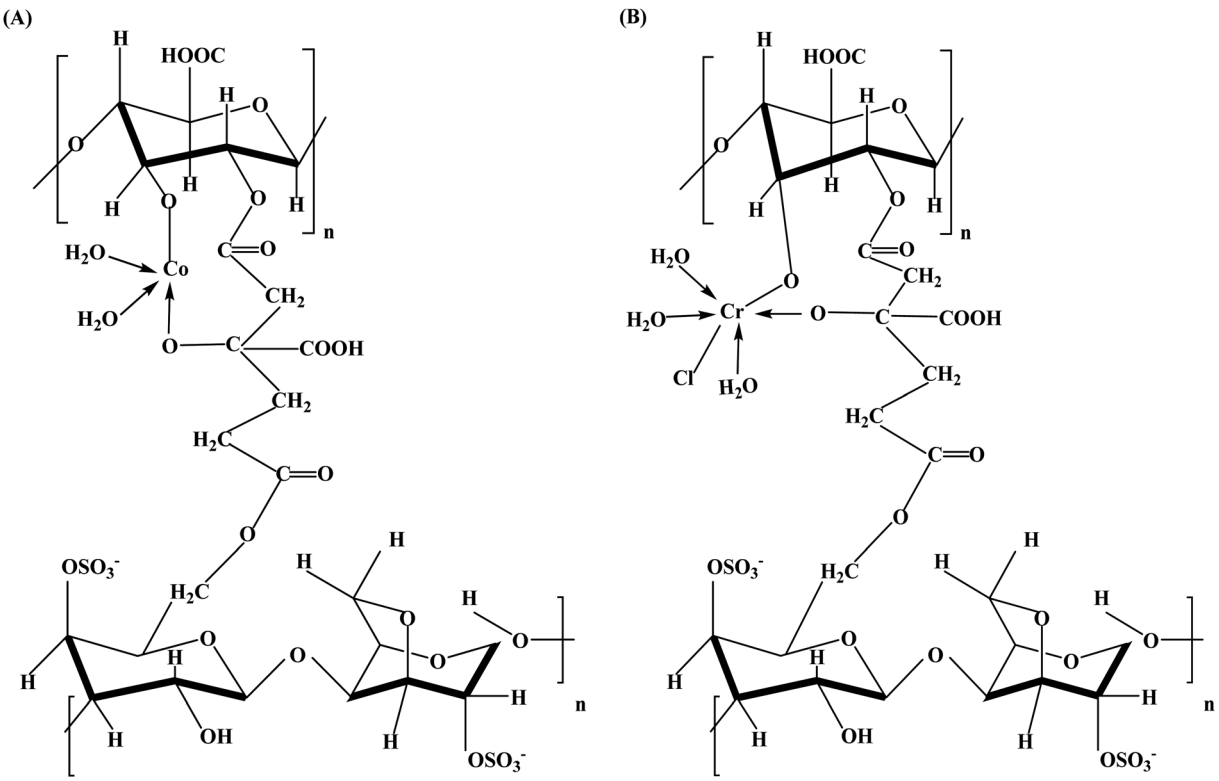

Fig. 2 Proposed structures of the complex (A) [Co(AG/CTR/CAR)$(H_2O)_2$], and the complex (B) [Cr(AG/CTR/CAR)$(H_2O)_3$Cl].

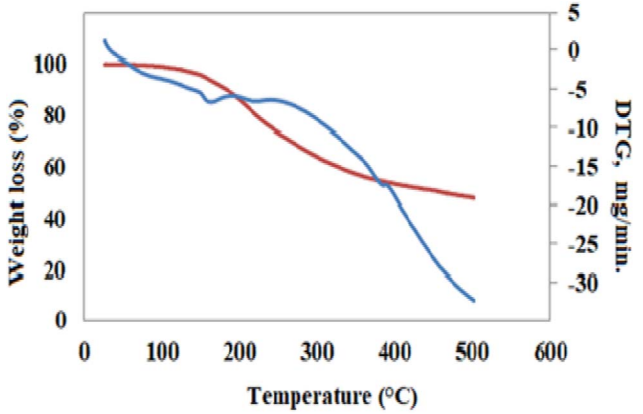

Fig. 3 TGA thermogram the Co(II) complex.

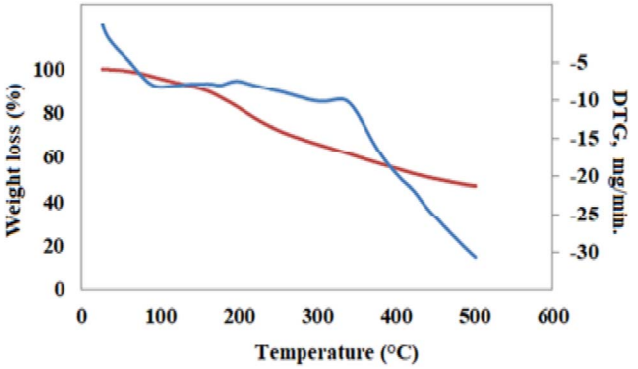

Fig. 4 TGA thermogram the of Cr(III) complex.

release of the two coordinated water molecules (theoretically 4.06%, practically 3.10%). The second step corresponds to the break of the TG bond (theoretically 19.96%, practically 18.60%). The third and fourth steps are connected with the decomposition of the rest of the compound and the weight loss was calculated to be 70. 09%, and the last one found at 70%. The rest of the complex thermally decomposes and cobalt oxide remains as a residue while the theoretical percentage is 8.40% and the obtained percentage is 8.90%.

Concerning the $Cr(AG/CTR/CAR)(H_2O)_3Cl$ polymeric complex, thermal analysis revealed 3 steps: 68–130 °C, 132–289 °C, and 291–550 °C. In the first stage 3 water molecules are lost (calculated 5. 75%, first stage found 4. 55%). The second stage is associated with the removal of chlorine wherein the calculated amount was 3. 77% while the experimental amount found was 3. 42%. The third weight loss was assigned to the decomposition of the other part of the compound. The stable final product that remained in the final stage was identified to be chromium oxide; its composition is calculated as 7.27% against the presence of 6.88% (Fig. 4).

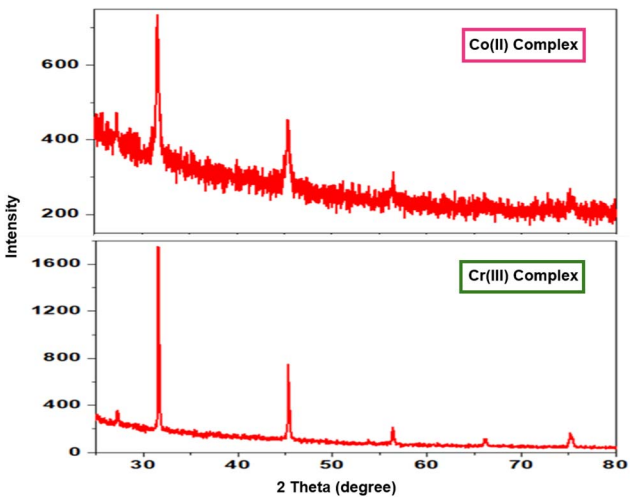

Fig. 5 XRD patterns of the different prepared polymeric complexes.

Crystallographic data of the polymeric compounds Co(II) and Cr(III) belong to the cubic tilted crystal system with the $Pm\bar{3}m$ space group (Table 5).

3.6. XRD Analysis of the polymeric complexes

Fig. 5 shows the different XRD patterns of the complexes. The results showed that the compounds were crystalline.

3.7. SEM morphological analysis

The morphological surface properties of the various produced polymeric complexes were investigated using SEM assessment.

Table 4 Thermal decomposition data for the different polymeric compounds[a]

	Temp. range (°C)			TGA (wt loss%)		
Complex	T_i	T_m	T_f	Calc. (%)	Found (%)	Assignment
Co(II) complex	80	116	125	4.05	3.76	Loss of two water molecules.
	127	188	214	19.69	18.83	Loss of ligand (AG)
	216	241	398	17.78	16.31	Loss of ligand (CAR)
	400	420	550	51.99	50.32	Loss of ligand (CT)
	—	—	—	15.06	14.26	The residue of cobalt oxide.
Cr(III) complex	68	113	130	5.77	4.03	Loss of three water molecules.
	132	222	289	3.79	18.86	Loss of chloride atom
	291	400	550	89.50	85.02	Loss of the rest of the ligand
	—	—	—	8.40	8.12	The residue chromium oxide.

[a] T_i = initial temperature, T_m = maximum temperature, T_f = final temperature.

Table 5 XRD crystal data of the different polymeric complexes (R_{wp}(%) = 6.49, R_{exp}(%) = 4.31, and R_B(%) = 1.03)[a]

Parameters	Co(II) complex	Cr(III) complex
Empirical formula	$C_{24}H_{29}O_{28}S_2Co$	$C_{24}H_{31}O_{29}S_2CrCl$
Formula weight	888.53	935.06
Crystal system	Cubic	Cubic
a (Å)	5.628	7.983
b (Å)	5.628	7.983
c (Å)	5.628	7.983
Alfa (°)	90.00	90.00
Beta (°)	99.74	90.00
Gamma (°)	90.00	90.00
Volume of unit cell (A^3)	178.29	508.7

[a] *a*, *b*, and *c* are the dimensions of the crystal system. Alfa, Beta, and Gamma are the angles of the crystal system of the different complexes.

Various magnifications were used to assess the surface characteristics and the effect of every kind of additional metal ion. As a general observation, Fig. 6 illustrates an apparent variation in surface morphology based on the metal type applied. The crosslinked polymeric ligand showed a porous and rough surface in every micrograph, indicating its improved hydrophilic characteristic. This surface property may be useful for the polymeric-metal complex formation process as well as for the subsequent uses of the complexes in different biological applications[41] Fig. 6-a shows the ideal shape of regular phase materials in the homogeneous matrix of Co(II) images. The Cr(III) complex showed a branched crack structure (Fig. 6-b).

3.8. Biological activity of the different polymeric compounds

3.8.1. Antimicrobial and antioxidant assays. The antimicrobial efficiency of the different polymer was evaluated against Gram negative and positive bacteria and a yeast *Candida albicans*. According the results summarized in the Table 6 and Fig. 7, the results demonstrate that all the tested complexes are active on bacteria and yeast and able to inhibit microbial growth. An interesting antibacterial effect was recorded with

Table 6 Antimicrobial and antioxidant activity of the ligand and the different polymeric complexes[a]

	Antimicrobial activity (inhibition zone (cm))					Antioxidant (%)
	Sa	Ml	Ec	St	Ca	
Ligand	0	0	0.95	1.05	0	95 ± 1.4
Co(II) complex	1.4	1	1.35	1.85	1.05	88 ± 0.7
Cr(III) complex	1.35	1.25	1.2	1.4	1.3	93 ± 1.4

[a] Sa: *Staphylococcus aureus* ATCC 25923; Ml: *Staphylococcus aureus* NCIMB 8166; Ec: *Escherichia coli* ATCC25922; St: *Salmonella typhimurium* ATCC 14080; Ca *Candida albicans* ATCC 90028.

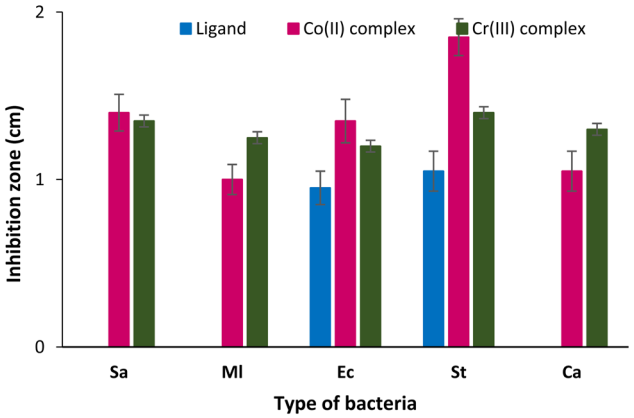

Fig. 7 Antibacterial and antifungal assessment of the ligand and the different polymeric complexes against various bacteria strains *via* the determination of the inhibition zone around samples. Sa: *Staphylococcus aureus* ATCC 25923; Ml: *Staphylococcus aureus* NCIMB 8166; Ec: *Escherichia coli* ATCC25922; St: *Salmonella typhimurium* ATCC 14080; Ca Candida albicans ATCC 90028.

Co(II) on *S. aureus* with an inhibitory zone of 14.5 mm and on *S. typhimurium* with a inhibitory area of 18.5 mm. The Cr(III) polymeric complex in turn showed a significant antibacterial performance on *S. aureus* with an inhibitory zone of 14.1 mm and on *S. typhimurium* with a inhibitory diameter of 14.2 mm.

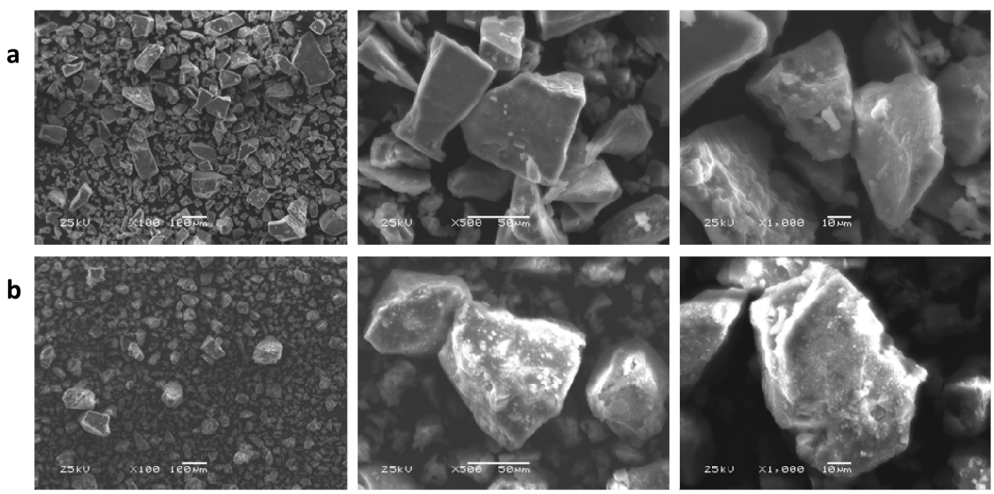

Fig. 6 SEM micrographs of the Co(II) (a) and Cr(III) (b) polymeric complexes at different magnifications.

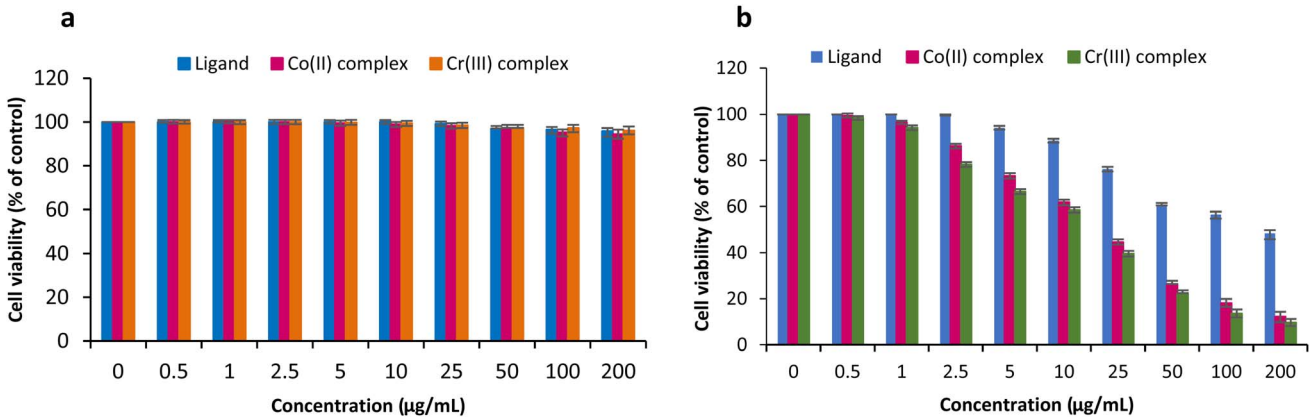

Fig. 8 Cell viability test in human normal breast cells (a) and anticancer activity in human breast cancer cells (b) of the ligand and the polymeric complexes *via* cell growth inhibition rates after 72 hours of incubation on MCF-7 and MCF-10A cell lines with varied concentrations.

The variation in the diameters of the zones of inhibition may be impacted by the microorganisms, and the antibacterial potential of the active substances of the complexes.

3.8.2. Antioxidant activity. Oxidative stress is a factious possibility to human health and is presumed as a sure index of cancer and chronic diseases. Patients' diseases are protected from advancement through the administration of antioxidant compounds. DPPH assessment is a fast and easy method that can conveniently assess the antioxidant activity and due to this, it is popularly considered to be the best method for evaluation of antioxidants from natural and synthetic sources. As described in Table 6, there was the apparent high antioxidant potential of all the two polymeric complexes under investigation. Indeed, the DPPH scavenging activity The DPPH reached 88% and 93% for the Co(II) and the Cr(III) polymeric complexes, respectively. The biopolymeric ligand has recorded a high antioxidant effect of 95%.

3.8.3. *In vitro* anticancer evaluation. The biocompatibility behavior and the anticancer activity of the prepared polymeric complexes were assessed *via* the *in vitro* cell tests. Human breast cancer cells (MCF-7) were exploited to evaluate the anticancer performance of the crosslinked natural ligand and its two metal complexes the poly-AG/CTR/CAR/Co(II) and the poly-AG/CTR/CAR/Cr(III). The assays were performed with varied concentrations of the polymers during the MTT test. The polymeric ligand in contact with normal epithelial cells did not cause any cytotoxicity, as seen in the results shown in Fig. 8-a. This is consistent with several published studies.[44,45] That validated the high biocompatibility of naturally derived polysaccharides. Thus, a safe drug delivery carrier made of a crosslinked polymer of alginate and carrageenan may be employed. The normal human breast epithelial cells (MCF10A) showed high cytocompatibility with both of the produced polymeric complexes of Co(II) and Cr(III) at different doses. This was an important breakthrough since the effectiveness of anticancer medications depends on how well they interact with the healthy cells that are the targets of the cancer. According to Fig. 8-b's anticancer evaluation, the polymeric ligand by itself was able to considerably destroy cancer cells at a dose of 50 μg mL^{-1}, and revealed an IC50 of 18.46 μg mL^{-1} corresponding to 23.2 μM. At 200 g mL^{-1}, the anticancer performance rises with sample concentration and reaches 44%. This result was in line with other research that was published in the literature.[46] In a dose-dependent manner, the two proposed complexes demonstrated substantial killing capacity against cancer cells. Similar to its antibacterial action, the Co(II) complex (IC50 = 10.12 μg mL^{-1} corresponding to 11.3 μM) performed worse against cancer than the Cr(III) complex (11.04 μg mL^{-1} corresponding to 11.8 μM). The metal complexation dramatically reduced the viability of MCF-7 cancer cells up to 8.2 ± 1.41% and 14.2 ± 1.64% for the Co(II) and Cr(III) complexes, respectively, after 72 hours of incubation and at a concentration of 200 μg mL^{-1}. When in the presence of normal human epithelial cells, the ligand and both complexes demonstrated good cytocompatibility overall. Additionally, the *in vitro* anticancer investigation showed the produced polymer complexes' strong anticancer capability, which was significantly enhanced with the used dose.

4. Conclusions

Further, it was observed that the cross-linked alginate/carrageenan biopolymer is a more suitable cross-linking agent for the synthesis of metal cations Co(II) and Cr(III). The ensuing polymeric complexes that had formed were analyzed by using IR, UV, TGA-DTA, XRD, and SEM. Upon analyzing the antimicrobial properties, it was observed that the various polymeric complexes revealed significant antibacterial and antifungal activities. The two synthesized polymeric complexes have shown an effective activity against both the Gram-positive and Gram-negative bacterial strains. Furthermore, the polymeric ligand and the prepared complexes demonstrated a high antioxidant performance. In fact, the DDPH analysis revealed that the two complexes were elite to scavenge free radicals and had a DPPH scavenging activity ranging from 88 to 95%. Viability tests showed that the polymeric crosslinked ligand comprising alginate and carrageenan had good cytocompatibility and could be used as a secure and reliable drug delivery vehicle. When

Co(II) and Cr(III) polymer complexes were exposed to normal human breast epithelial cells (MCF10A), they did not show any cytotoxicity. Additionally, using human breast cancer cells (MCF-7), they demonstrated anticancer activity that increases considerably with dose, with respective IC50 values of 10.12 (11.3 μM) and 11.04 μg mL^{-1} (11.8 μM) for Co(II) and Cr(III) complexes, respectively. Additional research studies on the antitumor potential of poly-AG/CTR/CAR/Co(II) and poly-AG/CTR/CAR/Cr(III) complexes in animal models are warranted.

Data availability

The authors confirm that the data supporting the findings of this study are available in the article.

Conflicts of interest

The authors declare no conflicts of interest.

Acknowledgements

The authors are thankful to the Deanship of Graduate Studies and Scientific Research at the University of Bisha for supporting this work through the Fast-Track Research Support Program.

References

1 A. Umemura, *et al.*, Morphology design of porous coordination polymer crystals by coordination modulation, *J. Am. Chem. Soc.*, 2011, **133**(39), 15506–15513.
2 L. Carlucci, C. Gianfranco and M. P. Davide, *Coordination polymers and supramolecular architectures book*, 1999.
3 J.-L. Du, *et al.*, *CrystEngComm*, 2008, **10**, 1866–1874.
4 X. Chen, B. Ye and M. Tong, *Coord. Chem. Rev.*, 2005, **249**, 545.
5 J. Bernstein, P. M. Fishbane and S. G. Gasiorowicz, *Modern Physics*, Prentice-Hall, 2000, vol. 3, p. 624.
6 J. Baranwal, B. Barse, A. Fais, G. L. Delogu and A. Kumar, Biopolymer: A Sustainable Material for Food and Medical Applications, *Polymers*, 2022, **14**, 983.
7 L. López-Hortas, N. Flórez-Fernández, M. D. Torres, T. Ferreira-Anta, M. P. Casas, E. M. Balboa, E. Falqué and H. Domínguez, Applying Seaweed Compounds in Cosmetics, Cosmeceuticals and Nutricosmetics, *Mar. Drugs*, 2021, **19**, 552.
8 M. S. Al-Fakeh, M. S. Alazmi and Y. EL-Ghoul, Preparation and characterization of nano-sized Co(II), Cu(II), Mn(II) and Ni(II) coordination PAA/Alginate biopolymers and study of their biological and anticancer performance, *Crystals*, 2023, **13**(7), 1148.
9 S. Lomartire, J. C. Marques and A. M. M. Gonçalves, An Overview of the Alternative Use of Seaweeds to Produce Safe and Sustainable Bio-Packaging, *Appl. Sci.*, 2022, **12**, 3123.
10 F. M. Almutairi, Y. El-Ghoul and M. Jabli, Extraction of Cellulose Polymeric Material from Populus tremula Fibers: Characterization and Application to the Adsorption of Methylene Blue and Crystal Violet, *Polymers*, 2021, **13**, 3334.
11 Z. Liu, T. Gao, Y. Yang, F. Meng, F. Zhan, Q. Jiang and X. Sun, Anti-Cancer Activity of Porphyran and Carrageenan from Red Seaweeds, *Molecules*, 2019, **24**, 4286.
12 A. Prasetyaningrum, D. P. Utomo, A. F. A. Raemas, T. D. Kusworo, B. Jos and M. Djaeni, Alginate/κ-Carrageenan-Based Edible Films Incorporated with Clove Essential Oil: Physico-Chemical Characterization and Antioxidant-Antimicrobial Activity, *Polymers*, 2021, **13**, 354.
13 Y. El-Ghoul and F. M. Alminderej, Bioactive and superabsorbent cellulosic dressing grafted alginate and Carthamus tinctorius polysaccharide extract for the treatment of chronic wounds, *Text. Res. J.*, 2021, **91**(3–4), 235–248.
14 K. S. Postolović, M. D. Antonijević, B. Ljujić, S. Radenković, M. Miletić Kovačević, Z. Hiezl, S. Pavlović, I. Radojević and Z. Stanić, Curcumin and Diclofenac Therapeutic Efficacy Enhancement Applying Transdermal Hydrogel Polymer Films, Based on Carrageenan, Alginate and Poloxamer, *Polymers*, 2022, **14**, 4091.
15 M. S. Al-Fakeh, N. F. Al-Otaibi and M. Alrasheedi, NA Alsaiari Synthesis, antimicrobial and antioxidant activities of ZnO, PbO, and Al_2O_3 NPs obtained by calcining new coordination polymers, *Results Chem.*, 2024, 101840.
16 Y. P. Yew, K. Shameli, S. E. Mohamad, K. X. Lee and S.-Y. Teow, Green Synthesized Montmorillonite/Carrageenan/Fe3O4 Nanocomposites for pH-Responsive Release of Protocatechuic Acid and Its Anticancer Activity, *Int. J. Mol. Sci.*, 2020, **21**, 4851.
17 Y. El-Ghoul, A. S. Altuwayjiri and G. A. Alharbi, Synthesis and characterization of new electrospun medical scaffold-based modified cellulose nanofiber and bioactive natural propolis for potential wound dressing applications, *RSC Adv.*, 2024, **14**(36), 26183–26197.
18 A. Boyd and A. M. Chakrabarty, Pseudomonas aeruginosa biofilms: role of the alginate exopolysaccharide, *J. Ind. Microbiol.*, 1999, **15**(3), 162–168.
19 L. Ding, X. Cui, R. Jiang, K. Zhou, Y. Wen, C. Wang, Z. Yue, S. Shen and X. Pan Design, Synthesis and Characterization of a Novel Type of Thermo-Responsible Phospholipid Microcapsule–Alginate Composite Hydrogel for Drug Delivery, *Molecules*, 2020, **25**, 694, DOI: **10.3390/molecules25030694**.
20 K. Y. Lee and D. J. Mooney, Alginate: properties and biomedical applications, *Prog. Polym. Sci.*, 2012, **37**, 106–126.
21 M. S. Al-Fakeh, N. Amiri, A. N. Al-Hakemi, S. E. S. Saeed and A. E. A. E. Albadri, Synthesis and properties of two Fe (III) coordination polymers based on 2-amino-4-methylthiazole, 2-mercaptobenzothiazole and aromatic polycarboxylate, *Asian J. Chem.*, 2020, **32**(10), 2502–2506.
22 G. Rassu, A. Salis, E. P. Porcu, P. Giunchedi, M. Roldo and E. Gavini, Composite chitosan/alginate hydrogel for controlled release of deferoxamine: a system to potentially treat iron dysregulation diseases, *Carbohydr. Polym.*, 2016, **136**, 1338–1347.

23 B. A. Harper, S. Barbut, L. T. Lim and M. F. Marcone, Effect of various gelling cations on the physical properties of "wet" alginate films, *J. Food Sci.*, 2014, **79**, E562–E567.
24 W. R. Gombotz and S. F. Wee, Protein release from alginate matrices, *Adv. Drug Deliv. Rev.*, 2012, **64**, 194–205.
25 P. Treenate and P. Monvisade, In vitro, drug release profiles of pH-sensitive hydroxyethylacryl chitosan/sodium alginate hydrogels using paracetamol as a soluble model drug, *Int. J. Biol. Macromol.*, 2017, **99**, 71–78.
26 J. G. Leid, C. J. Willson, M. E. Shirtliff, D. J. Hassett, M. R. Parsek and A. K. Jeffers, The exopolysaccharide alginate protects Pseudomonas aeruginosa biofilm bacteria from IFN-gamma-mediated macrophage killing, *J. Immunol.*, 2005, **175**(11), 7512–7518, DOI: **10.4049/jimmunol.175.11.7512**.
27 M. Younes, P. Aggett, F. Aguilar and R. Crebelli, Re-evaluation of carrageenan (E 407) and processed Eucheuma seaweed (E 407a) as food additives, *EFSA J.*, 2018, **16**(4), DOI: **10.2903/j.efsa.2018.5238**.
28 K. Mahmood Zia, S. Tabasum, M. Nasif and M. Zuber, A review on synthesis, properties and applications of natural polymer based carrageenan blends and composites, *Int. J. Biol. Macromol.*, 2017, **96**(3), 282–301.
29 S. Kraan, Algal polysaccharides, novel applications and outlook, in *Carbohydrates; comprehensive studies on glycobiology and glycotech-nology*, ed. C. FaChang, 1st edn, 2012, vol. 99, pp. 489–532.
30 Y. EL-Ghoul, M. S. Al-Fakeh and N. S. Al-Subaie, Synthesis and Characterization of a New Alginate/Carrageenan Crosslinked Biopolymer and Study of the Antibacterial, Antioxidant, and Anticancer Performance of Its Mn(II), Fe(III), Ni(II), and Cu(II) Polymeric Complexes, *Polymers*, 2023, **15**(11), 2511.
31 G. Jiao, G. Yu, J. Zhang and H. S. Ewart, *Mar. Drugs*, 2011, **9**, 196–223.
32 J. Necas and L. Bartosikova, *Vet. Med*, 2013, **58**, 187–205.
33 M. S. Al-Fakeh, M. Alrasheedi, A. E. M. E. Mohammed, A. B. M. Ibrahim, S. M. Al-Hazmy, I. A. Alhagri and S. Messaoudi, Synthesis, Characterization, DNA, Fluorescence, Molecular Docking, and Antimicrobial Evaluation of Novel Pd(II) Complex Containing O, S Donor Schiff Base Ligand and Azole Derivative, *Inorganics*, 2024, **12**, 7.
34 D. V. Prajapati, P. M. Maheriya, G. K. Jani and H. K. Solanki, *Carbohydr. Polym.*, 2014, **105**, 97–112.
35 A. P. Imeson, Carrageenan, in *Handbook of hydrocolloids*, ed. G. O. Phillips and P. A. Williams, Woodhead Publishing Limited, Cambridge, UK, 2000, pp. 87–102.
36 A. Dbeibia, F. Ben Taheur, K. A. Altammar, N. Haddaji, A. Mahdhi, Z. Amri, R. Mzoughi and C. Jabeur, Control of Staphylococcus aureus methicillin resistant isolated from auricular infections using aqueous and methanolic extracts of Ephedra alata, *Saudi J. Biol. Sci.*, 2021, **29**, 1021–1028.
37 W. Piang-Siong, P. de Caro, A. Marvilliers, X. Chasseray, B. Payet, A. Shum Cheong Sing and B. Illien, Contribution of trans-aconitic acid to DPPH scavenging ability in different media, *Food Chem.*, 2017, **214**, 447–452.
38 M. Ahamed, M. Akhtar, M. A. Siddiqui, J. Ahmad, J. Musarrat, A. A. Al-Khedhairy, M. AlSalhi and S. A. Alrokayan, Oxidative stress mediated apoptosis induced by nickel ferrite nanoparticles in cultured A549 cells, *Toxicology*, 2011, **283**, 101–108.
39 M. R. Kasaai, A review of several reported procedures to determine the degree of N-acetylation for chitin and chitosan using infrared spectroscopy, *Carbohydr. Polym.*, 2008, **71**, 497–508.
40 C. Rochas, M. Lahaye and W. Yaphe, Sulfate Content of Carrageenan and Agar Determined by Infrared Spectroscopy, *Bot. Mar.*, 1986, **29**, 335–340.
41 M. S. Al-Fakeh, M. A. Alsikhan and J. Sh Alnawmasi, Physico-Chemical Study of Mn(II), Co(II), Cu(II), Cr(III), and Pd(II) Complexes with Schiff-Base and Aminopyrimidyl Derivatives and Anti-Cancer, Antioxidant, Antimicrobial Applications, *Molecules*, 2023, **28**(6), 2555.
42 M. S. Al-Fakeh, S. Messaoudi, F. I. Alresheedi, A. EAE Albadri, W. A. El-Sayed and E. E. Saleh, Preparation, Characterization, DFT Calculations, Antibacterial and Molecular Docking Study of Co (II), Cu (II), and Zn (II) Mixed Ligand Complexes, *Crystals*, 2023, **13**(1), 118.
43 M. S. Al-Fakeh and N. F. Al-Otaibi, Nd_2O_3, Cr_2O_3, and V_2O_3 Nanoparticles via Calcination: Synthesis, Characterization, Antimicrobial and Antioxidant Activities, *J. Nanotechnol.*, 2022, **2022**, 7794939.
44 R. Geetha Bai and R. Tuvikene, Potential Antiviral Properties of Industrially Important Marine Algal Polysaccharides and Their Significance in Fighting a Future Viral Pandemic, *Viruses*, 2021, **13**, 1817.
45 C. Liu, F. Jiang, Z. Xing, L. Fan, Y. Li, S. Wang, J. Ling and X.-K. Ouyang, Efficient Delivery of Curcumin by Alginate Oligosaccharide Coated Aminated Mesoporous Silica Nanoparticles and In Vitro Anticancer Activity against Colon Cancer Cells, *Pharmaceutics*, 2022, **14**, 1166.
46 A. G. Gutiérrez-Rodríguez, C. Juárez-Portilla, T. Olivares-Bañuelos and R. C. Zepeda, Anticancer activity of seaweeds, *Drug Discovery Today*, 2018, **23**(2), 434–447.